Vortex Softening: Origin of the Second Peak Effect in $Bi_2Sr_2CaCu_2O_{8+\delta}$

V. F. Correa, G. Nieva, and F. de la Cruz

Comisión Nacional de Energía Atómica, Centro Atómico Bariloche, 8400 S.C. de Bariloche, Argentina

(Received 24 November 2000; published 13 July 2001)

Magnetic hysteresis and transverse ac permeability measurements in $Bi_2Sr_2CaCu_2O_{8+\delta}$ allow a comparative analysis of the critical current with the elastic response of vortex structures, in equilibrium with their pinning potential, in the field and temperature region where the second peak is detected. This study provides strong evidence that the second peak has its origin in changes of the elastic equilibrium properties of the vortex structures.

DOI: 10.1103/PhysRevLett.87.057003 PACS numbers: 74.60.Ec, 74.60.Ge, 74.60.Jg, 74.72.Hs

The existence of the second peak in the low field, low temperature magnetization of $Bi_2Sr_2CaCu_2O_{8+\delta}$ (Bi2212) as well as the peak effect observed in the critical current J_c of low (LTS) and high temperature superconductors are manifestations of instabilities of the vortex structure (VS) in the presence of pinning potentials. Since the first explanation by Pippard and the theoretical description by Larkin and Ovchinnikov [1], several other alternatives have been proposed, including order/disorder thermodynamic phase transitions [2–6].

The most remarkable manifestation in both phenomena is that J_c goes through a maximum when increasing field. Thus, most experiments studying the anomaly are based on measurements of J_c and consequently describe the properties of a nonequilibrium thermodynamic state. In particular, in the case of the second peak in Bi2212, J_c determined by magnetization loop measurements is strongly affected by time dependent phenomena. As a result, it has been suggested [7] that a possible explanation for the second peak effect is the different relaxation rates of the vortex system in a nonhomogeneous field distribution induced by the critical state. Another suggestion supporting the dynamical origin of the phenomenon was introduced [8] from local magnetization loops induced in short time scales. This is in contrast with other experiments in Bi2212, where a thermodynamic phase transition is claimed [2–6] to be associated with the second peak.

In this paper we compare experimental results obtained by different techniques in order to distinguish the possible dynamical contribution to the second peak from that caused by genuine changes in the elastic response of the VS. We have compared magnetization loop measurements in the critical state with results obtained from the ac transverse permeability of vortex configurations free of bulk magnetic gradients. With this last constraint we were able to detect an enhancement of the intrinsic pinning potential of the vortex lattice in a region of fields where the second peak is detected. We suggest that this behavior is due to a softening of the elastic properties of vortices that might be considered a precursor of a phase transition.

The Bi2212 single crystals used in this paper were grown using the self-flux technique [9] and they have typical dimensions $2 \times 1 \times 0.02$ mm^3. We made measurements of the field cooled (FC) ac transverse permeability in the Campbell limit, where the VS remains pinned under the perturbation induced by the ac field. A sketch of the experimental configuration with the applied field H_a in the c direction can be seen in the inset of Fig. 1 and details in Ref. [10]. We used a frequency of 916 Hz and an h_{ac} amplitude of 0.1 Oe.

The ac permeability in this configuration is given [11] by

$$\mu = \frac{2\lambda_{ac}}{d}\tanh\left(\frac{d}{2\lambda_{ac}}\right), \tag{1}$$

where d is the thickness of the sample and the ac penetration depth λ_{ac} in the Campbell limit follows expression [11]

$$\lambda_{ac}^2 = \lambda_{ac}^2(H_a = 0) + \lambda_C^2, \tag{2}$$

where λ_C is the Campbell penetration depth. The Campbell limit is achieved when the ac response is characterized [12] by vortices locked in a pinning potential, linear frequency independent response to ac excitations, and a very

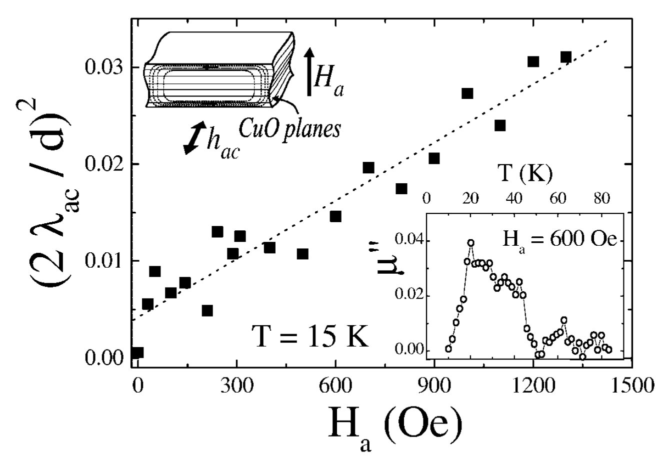

FIG. 1. Field dependence of λ_{ac}^2 at 15 K, normalized by the thickness of the sample. The dotted line is a linear fit to the data. Inset at the lower right: imaginary part of the permeability vs T at $H_a = 600$ Oe. Inset at the upper left: experimental configuration.

small dissipation due to the displacement of the vortex core within the effective pinning potential. The Campbell penetration depth is given by [11]

$$\lambda_C^2(H_a, T) = \frac{c_{44}}{\alpha_L(H_a, T)}, \quad (3)$$

where c_{44} is the tilting elastic constant and $\alpha_L(H_a, T)$ is the effective pinning potential (Labusch parameter).

When the only external force applied to the VS is that of the perturbation induced by the ac field the elastic response in the Campbell limit is determined by the curvature at the bottom of the effective pinning potential. This requires the electromagnetic force induced by the ac field to be much smaller than the critical force to remove vortices from the pinning sites. Basically, the VS localized at the bottom of the Labusch potential represents a free force VS in thermodynamic equilibrium with the pinning potential. In practice, the true equilibrium state for a given external field and temperature cannot be reached. On the other hand, the structure obtained by freezing the FC vortex system through the liquid-solid first order transition is essentially a vortex free force configuration down to temperatures where the single vortex limit is achieved [13]. In this configuration the pinning barrier is maximum [14] and, in the single vortex pinning limit, $\alpha_L(H_a, T)$ becomes field independent. In this limit, the field dependence of $\lambda_C^2 = H_a \phi_0 / 4\pi \alpha_L(T)$ is given by the field dependence of $c_{44} = H_a \phi_0 / 4\pi$ (defined in units of energy per vortex unit length). Typically, when the field is increased the vortex-vortex interaction becomes relevant and a crossover to the collective pinning regime takes place. Then $\alpha_L(H_a, T)$ decreases, and the Campbell penetration depth increases.

Magnetization loops were also measured using a commercial quantum design SQUID magnetometer. From these measurements J_c was extracted by using the expression [15]

$$J_c = \frac{3}{2} \frac{c \Delta M}{R}, \quad (4)$$

where ΔM is the difference in magnetization for a given field and R is a typical dimension of the sample. Equation (4) gives J_c only when creep effects can be disregarded. In this case [16], $J_c \propto \alpha_L(H_a, T)$. The measurements were taken in a time scale of a few minutes.

In Fig. 1 we show the field dependence of λ_{ac}^2 at 15 K, normalized by the thickness of the sample. The imaginary part of the permeability shows the low dissipation peak corresponding to the Campbell limit (see the inset at the lower right of Fig. 1). The linear dependence of λ_{ac}^2 with H_a confirms the single vortex limit up to fields as high as 1500 Oe.

The field independent Labusch coefficient is obtained from

$$\alpha_L = \frac{H_a \phi_0}{4\pi} [\lambda_{ac}^2(H_a, T) - \lambda_{ac}^2(0, T)]^{-1}, \quad (5)$$

where $\lambda_{ac}(0, T)$ obtained from the extrapolation of the linear field dependence is larger $[\lambda_{ac}(0, T) \approx 3\lambda_L]$ than the London penetration depth λ_L, as observed in other materials [17]. The slope of $\lambda_{ac}^2(H_a, T)$ determines $\alpha_L(H_a, T)$, plotted as a solid line in Fig. 2, together with the corresponding values obtained from expression (5).

The current density J_c, obtained from (4) is also plotted in Fig. 2. It is interesting to point out that the J_c field independent region (single vortex regime) is limited to fields 1 order of magnitude smaller than those where α_L is seen to remain constant. Creep measurements [18] in the critical state made in the time scale of the same order of that used in the magnetization measurements show that the decrease of J_c as seen in Fig. 2 can be taken into account by creep effects. Equivalent measurements in the FC structure [18] show undetectable creep, in agreement with the results of decoration experiment [13] and with the observed constant $\alpha_L(H_a, T)$ plotted in Fig. 2.

Figure 3 depicts the field dependence of λ_{ac}^2 for three higher temperatures. The frequency independence of the results and the low dissipation ($\mu'' < 0.04$) verify that the Campbell limit is obeyed up to 750 Oe, where dissipation increases rapidly with field (shadowed region in the figure). The slope of $\lambda_{ac}^2(H_a, T)$ for the three temperatures is seen to be independent of field (indicated by the dash-dotted line with slope 1) for $H_a < 200$ Oe. It is interesting to notice the relative decrease of $\lambda_{ac}^2(H_a, T)$ with field as compared to that of the single vortex limit (followed by an increase at higher fields [19], shadowed region in the figure). It is surprising that the enhancement of the effective pinning potential (better shielding) with H_a takes place when the single vortex limit is dominant. This is seen in Fig. 4, where we have plotted $\alpha_L(H_a, T)$ from the data in Fig. 3, for two temperatures.

Critical currents extracted from magnetization loops for $T = 25$ and 35 K, together with the corresponding $\alpha_L(H_a, T)$ from permeability measurements, are shown in Fig. 4. As observed at lower temperatures, the decrease of J_c in the region of fields where α_L is field independent is also due to creep effects. Creep becomes more and more

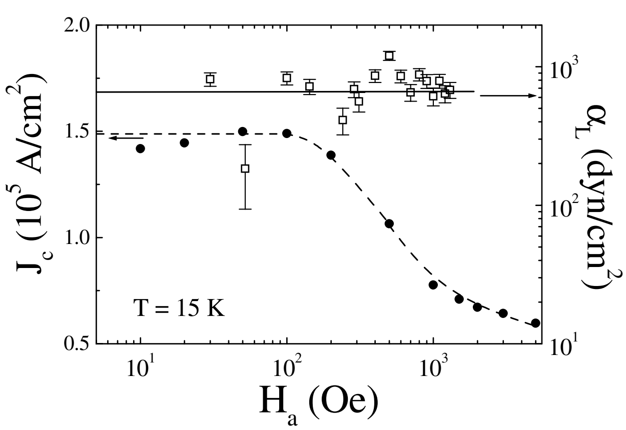

FIG. 2. J_c from magnetization loops and Labusch coefficient α_L from Eq. (5) as a function of the applied magnetic field. The lines are a guide to the eye for J_c data and the α_L value from the fit in Fig. 1.

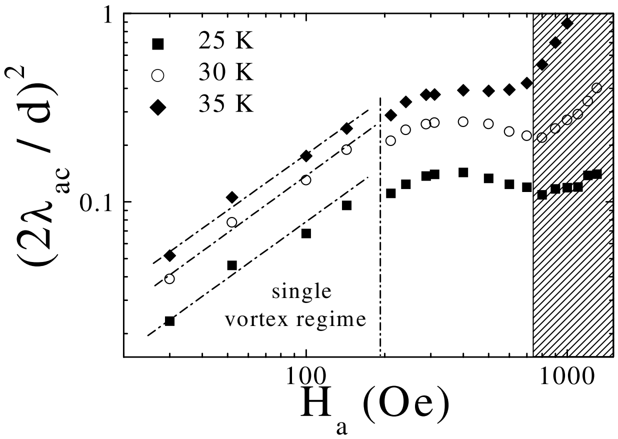

FIG. 3. Field dependence of λ_{ac}^2 at 25, 30, and 35 K. The shadowed region corresponds to a dissipative regime. The lines have slope 1, indicating a single vortex limit.

relevant in the magnetization loop measurements as the temperature increases. The increase of α_L in the creep-free experiment shows, however, nondramatic effects with temperature. The decrease in J_c with H_a should not be considered as an increase of the pinning correlation volume with field due to collective pinning effects and, consequently, should not be associated with the second peak effect. This is further supported by a close inspection

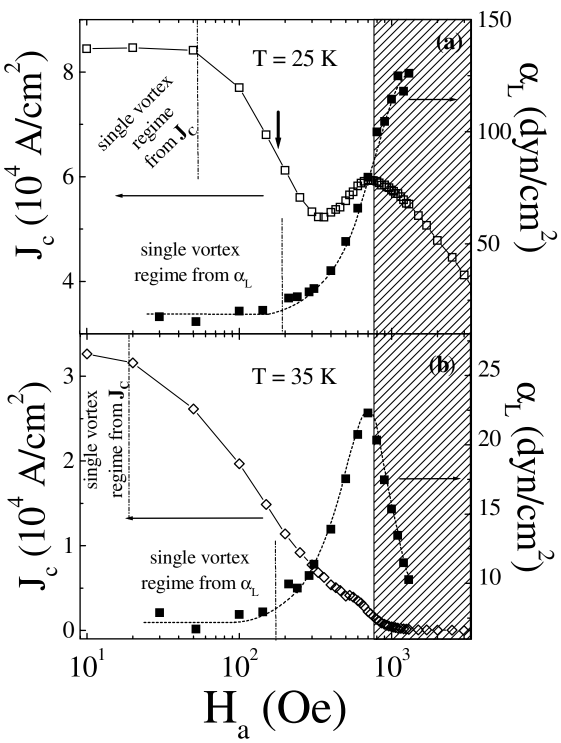

FIG. 4. J_c from magnetization loops and Labusch coefficient α_L from Eq. (5) as a function of the applied magnetic field for (a) $T = 25$ K and (b) $T = 35$ K. The single vortex region (field independence) deduced for both magnitudes is indicated. The arrow marks the inflection point of $J_c(H_a)$. The shadowed region corresponds to a dissipative regime.

of the data in Fig. 4, showing that the enhancement of $\alpha_L(H_a, T)$ above the single vortex limit takes place at the field where the decreasing $J_c(H_a)$ shows an inflection point, as marked in the figure with an arrow. At this field a mechanism that increases $\alpha_L(H_a, T)$ is switched on and, consequently, slows down the creep rate. This anomalous behavior of the pinning potential appears as a precursor of the second peak effect.

It is interesting to point out similarities and differences between the peak effect close to $H_{c2}(T)$ in LTS [1,20], and the second peak in Bi2212 at low fields and temperatures. In LTS, J_c decreases with field down to a minimum at H_{onset}, then pinning increases to reach a maximum at H_{peak}. It is shown [20] that H_{onset} is situated in the field region, where collective pinning is described by a three-dimensional Larkin volume. For $H_a > H_{\text{onset}}$ the correlation volume decreases until a crossover from the collective to the single vortex limit takes place at H_{peak}. The previous description implies that $\alpha_L(H_a, T)$ decreases down to a minimum at $H_a = H_{\text{onset}}$. The enhancement of $\alpha_L(H_a, T)$ for $H_a > H_{\text{onset}}$ indicates a reduction of the correlation volume induced by a softening of the VS. Agreement between theory and experiment is found [20] only if the pinning correlation volume is calculated, taking into account the lattice softening induced by the dispersive nature of $c_{44}(k)$. This is important close to H_{c2} where the typical interaction length $\lambda_H = \lambda_L/1 - b$ ($b = H/H_{c2}$) becomes comparable to the relevant elastic distortion of wave vector k of the VS.

In the extreme anisotropic Bi2212, pinning is also shown to increase with field at the second peak. However, in this case $\alpha_L(H_a, T)$ shows no detectable minimum; it increases from a field independent value at low fields, as shown by penetration depth measurements. Thus the reduction of the vortex pinning correlation starts from the Larkin volume in the single vortex limit, characterized by a one-dimensional vortex length, L_c. In this limit J_c is given by [1]

$$J_c = J_0(T)\left(\frac{\xi(T)}{L_c(T)\gamma}\right)^2, \tag{6}$$

where $J_0(T)$ is the depairing current, ξ is the superconducting coherence length, γ is the anisotropy, and L_c is the Larkin correlation length in the field direction. Previous measurements of J_c and $\alpha_L(H_a, T)$ have shown [21] a field independent, temperature-induced crossover from one- to zero-dimensional pinning behavior at $T_{0D} \simeq 20$ K, where L_c becomes equal [21] to the CuO interspacing distance s.

The temperature dependence of $\alpha_L(H_a, T)$ in the single vortex limit is depicted in Fig. 5. The transition to the zero-dimensional limit, $T = T_{0D}$, is evident [21]. At this temperature the minimum pinning correlation volume [maximum $\alpha_L(H_a, T)$ for a given temperature] is achieved. For $T > 20$ K the pinning is one dimensional with $L_c > s$. Thus, the increase of $\alpha_L(H_a, T)$ with field, described in this paper, should be due to a decrease of L_c induced by a softening of the elastic vortex properties. Following the previous discussion the maximum value that

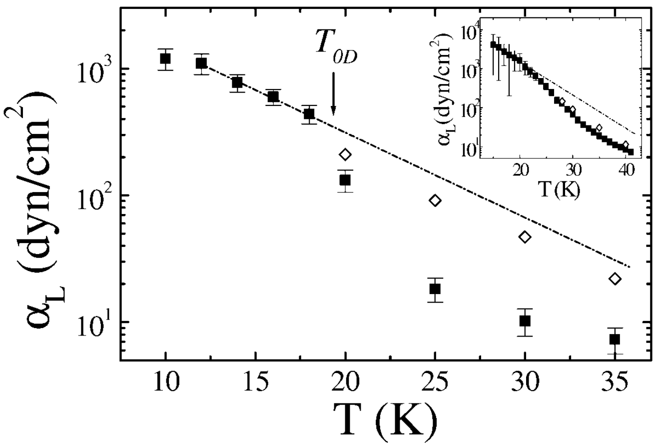

FIG. 5. Temperature dependence of $\alpha_L(H_a, T)$ in the single vortex limit. Filled symbols: field independent α_L. Open symbols: largest value of α_L in the Campbell limit. The dash-dotted line is an extrapolation of the low temperature (below T_{0D}) evolution. The inset is a similar result for a sample with lower defect concentration.

$\alpha_L(H_a, T)$ can take is that for $L_c = s$. We have plotted in Fig. 5 the largest values of $\alpha_L(H_a, T)$ at different temperatures within the Campbell limit (for fields H_a in Fig. 4 smaller than those in the shadowed area). The linear extrapolation (dash-dotted line) of the data below 20 K to higher temperatures is never surpassed by the largest values of $\alpha_L(H_a, T)$ obtained in the experiments within the Campbell regime, strongly supporting the picture discussed previously.

It is seen from Fig. 5 that the increase of $\alpha_L(H_a, T)$ and the corresponding increase of $J_c(H_a, T)$ at the second peak is due to a softening of the elastic properties of the vortices in a region of fields where its integrity along the field is ensured: single vortex limit in the Campbell regime. When H_a is further increased, J_c and the effective $\alpha_L(H_a, T)$ are seen to decrease rapidly but the rapid increase of dissipation in μ indicates a crossover to a nonequilibrium state. The large dissipation is associated with currents flowing in the c direction, as mentioned in Ref. [10], indicating a loss of vortex integrity in transport properties.

We have made measurements in two other samples with similar results. However, it is interesting to remark that the field where dissipation marks the end of the Campbell limit depends on each sample, i.e., for the sample shown in the inset of Fig. 5 (that by all indications seems to be cleaner) the dissipation appears at values of $\alpha_L(H_a, T)$ well below that corresponding to the zero pinning limit behavior. This result is in agreement with a possible influence of point disorder on a first order transition associated with the loss of coherence in the c direction.

We have shown that the increase of J_c in the second peak effect is due to a genuine softening of the elastic properties in the dominant single vortex regime. Whether it is a manifestation of a phase transition is a subject that deserves more theoretical and experimental work.

V. F. C. and G. N. thank CONICET, Argentina for its support. Work is partially supported by ANPCYT PICT97-03-00061-01116, CONICET PIP96/4207, Fundación Balseiro, and Fundación Antorchas 1370/1-1118.

[1] A. I. Larkin and Yu. N. Ovchinnikov, J. Low Temp. Phys. **34**, 409 (1979).
[2] T. Giamarchi and P. Le Doussal, Phys. Rev. B **52**, 1242 (1995).
[3] L. L. Daemen *et al.,* Phys. Rev. Lett. **70**, 1167 (1993).
[4] E. Zeldov *et al.,* Europhys. Lett. **30**, 367 (1995).
[5] M. B. Gaifullin *et al.,* Phys. Rev. Lett. **84**, 2945 (2000).
[6] B. Horovitz, Phys. Rev. B **60**, R9939 (1999).
[7] M. Nideröst *et al.,* Phys. Rev. B **53**, 9286 (1996).
[8] M. Baziljevich *et al.,* Phys. Rev. B **62**, 4058 (2000), and references therein.
[9] E. E. Kaul and G. Nieva, Physica (Amsterdam) **341C–348C**, 1343 (2000).
[10] A. Arribere *et al.,* Phys. Rev. B **48**, 7486 (1993).
[11] E. H. Brandt, Phys. Rev. Lett. **67**, 2219 (1991).
[12] A. M. Campbell, J. Phys. C **2**, 1492 (1969).
[13] Magnetic decoration experiments of FC vortex structures show no field gradients in the bulk of the sample. This imposes a maximum limit of less than $J = 10$ A/cm^2 (we thank Y. Fasano for this information).
[14] G. Blatter *et al.,* Rev. Mod. Phys. **66**, 1125 (1994).
[15] C. P. Bean, Rev. Mod. Phys. **36**, 31 (1964).
[16] A. M. Campbell and J. E. Evetts, Adv. Phys. **21**, 199 (1972).
[17] G. Pasquini *et al.,* Phys. Rev. B **59**, 9627 (1999); G. Pasquini, Ph.D. thesis, Universidad Nacional de Buenos Aires, 1998 (unpublished).
[18] V. F. Correa *et al.* (unpublished).
[19] M. F. Goffman *et al.,* Phys. Rev. B **57**, 3663 (1998).
[20] L. A. Angurel *et al.,* Phys. Rev. B **56**, 3425 (1997).
[21] V. F. Correa *et al.,* Phys. Rev. B **63**, 92 502 (2001).